Available online at www.sciencedirect.com
ScienceDirect
Proceedings of the Combustion Institute 32 (2009) 2727–2742
Proceedings of the Combustion Institute
www.elsevier.com/locate/proci

Advanced compression-ignition engines—understanding the in-cylinder processes

John E. Dec *

Sandia National Laboratories, MS 9053, P.O. Box 969, Livermore, CA 94551-0969, USA

Abstract

Advanced compression-ignition (CI) engines can deliver both high efficiencies and very low NO_X and particulate (PM) emissions. Efficiencies are comparable to conventional diesel engines, but unlike conventional diesel engines, the charge is highly dilute and premixed (or partially premixed) to achieve low emissions. Dilution is accomplished by operating either lean or with large amounts of EGR. The development of these advanced CI engines has evolved mainly along two lines. First, for fuels other than diesel, a combustion process commonly known as homogeneous charge compression-ignition (HCCI) is generally used, in which the charge is premixed before being compression ignited. Although termed "homogeneous," there are always some thermal or mixture inhomogeneities in real HCCI engines, and it is sometimes desirable to introduce additional stratification. Second, for diesel fuel (which autoignites easily but has low volatility) an alternative low-temperature combustion (LTC) approach is used, in which the autoignition is closely coupled to the fuel-injection event to provide control over ignition timing. To obtain dilute LTC, this approach relies on high levels of EGR, and injection timing is typically shifted 10–15° CA earlier or later than for conventional diesel combustion so temperatures are lower, which delays ignition and provides more time for premixing. Although these advanced CI combustion modes have important advantages, there are difficulties to implementing them in practical engines. In this article, the principles of HCCI and diesel LTC engines are reviewed along with the results of research on the in-cylinder processes. This research has resulted in substantial progress toward overcoming the main challenges facing these engines, including: improving low-load combustion efficiency, increasing the high-load limit, understanding fuel effects, and maintaining low NO_X and PM emissions over the operating range.

Keywords: Compression-ignition; Engines; HCCI; LTC; In-cylinder

1. Introduction

With concerns about limited petroleum supplies and global warming driving the demand for fuel-efficient engines, interest in compression-ignition (CI) engines is stronger than ever. CI engines are the most fuel-efficient engines ever developed for transportation purposes, due largely to their relatively high compression ratios and lack of throttling losses. However, conventional CI diesel engines have relatively high emissions of nitric oxides (NO_X) and particulate matter (PM). Although these emissions have been significantly reduced in recent years, further reductions are required to meet the very stringent US-2010 regulations [1] and beyond. At the same time, there is a

* Fax: +1 925 294 1004.
E-mail address: jedec@sandia.gov

1540-7489/$ - see front matter © 2009 The Combustion Institute. Published by Elsevier Inc. All rights reserved.
doi:10.1016/j.proci.2008.08.008

need for even higher efficiency, and the market requires that this be done with minimal cost.

Meeting the current emission regulations for diesel engines has required the development of a thorough understanding of the in-cylinder processes. To accomplish this, numerous investigations were conducted using advanced laser-imaging diagnostics. These studies provided a greatly improved understanding of diesel combustion, which is summarized by the schematic in Fig. 1 [2]. Guided by this understanding, diesel emissions have been reduced substantially over the past decade and a half with a minimal loss in engine efficiency. However, Fig. 1 also shows the factors that limit the reduction of emissions with traditional diesel combustion. The fuel and air first react in a fuel-rich mixture, leading to soot formation, then this rich mixture burns out in a high-temperature diffusion flame at the jet periphery, leading to NO_X formation [3]. Nevertheless, advanced combustion systems with increased injection pressure, EGR, improved piston-bowl geometries, and improved in-cylinder flows have resulted in substantial reductions in emissions, and research efforts continue. Despite these efforts, it appears unlikely that conventional jet-mixing controlled diesel combustion can meet future emission requirements without fairly expensive aftertreatment systems.

To address the combined needs of further emissions reduction, improved efficiency, and cost, engine-combustion researchers and development engineers are turning to alternative forms of CI combustion. Various methods are being pursued, but they all rely on the principle of dilute premixed or partially premixed combustion to reduce emissions. This approach is exemplified by a technique commonly known as homogeneous charge compression-ignition (HCCI) [4]. In HCCI, the fuel and air are premixed and compression ignited; however, the mixture is made very dilute either by being lean with fuel/air equivalence ratios (ϕ) typically less than 0.45, or through the use of high levels of EGR for equivalence ratios up to stoichiometric [4–7]. Although these mixtures are typically too dilute to support flame-type combustion, they react and burn volumetrically as they are compressed to autoignition temperatures by the piston. Because of the high dilution, combustion temperatures are low, resulting in low NO_X emissions, and the charge is sufficiently well-mixed to prevent soot formation. Thermal efficiencies are typically comparable to those of a diesel engine [4,6–9]. Because of these advantages, substantial research and development efforts on HCCI are underway using a variety of fuels, including gasoline, diesel fuel, ethanol, natural gas, and others [4–12].

With diesel fuel, however, classic HCCI is not readily implemented due to the fuel's low volatility and the ease with which it autoignites (high cetane number) [4,8,12–15]. Therefore, many diesel-engine manufacturers and researchers are pursuing alternative approaches to achieve HCCI-like combustion, commonly referred to as diesel low-temperature combustion (LTC). With diesel LTC, various techniques are applied to obtain sufficient premixing so that combustion temperature and equivalence ratio combinations that lead to soot and NO_X formation are avoided. This is most easily understood by the ϕ-temperature diagram in Fig. 2 [16–18]. The diagram shows contour plots of the ϕ-temperature combinations at which soot and NO_X formation occur. As can be seen, the adiabatic flame temperature in air for typical diesel conditions traverses both the soot and NO_X formation regions. In conventional diesel combustion (Fig. 1), the fuel and air first react in a rich mixture at about $\phi = 4$, and then combustion goes to completion in a stoichiometric ($\phi = 1$) diffusion flame. Assuming that the combustion is nearly adiabatic, Fig. 2 shows that these combustion zones fall in the soot and NO_X

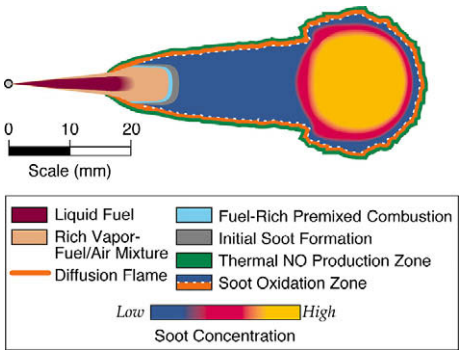

Fig. 1. Conceptual schematic of conventional diesel combustion, from [2].

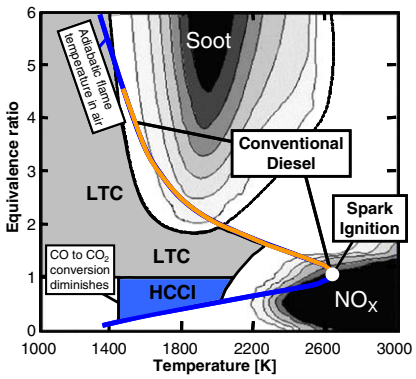

Fig. 2. Diagram showing the ϕ-temperature ranges for soot and NO_X formation and the regions for conventional diesel, SI, HCCI, and diesel LTC engines. Adapted from [16–18].

regions, respectively, leading to high levels of emissions. As evident in Fig. 2, spark-ignition (SI) combustion also produces considerable engine-out NO_X emissions, but they are readily removed by modern three-way catalysts.[1] However, SI engines have significantly lower thermal efficiencies than CI engines due to their lower compression ratios and throttling losses. Also shown in Fig. 2 is the HCCI combustion region, which falls outside the soot– and NO_x–formation regions. However, it is not necessary for combustion to occur exclusively in the HCCI region to avoid soot and NO_X. LTC diesel takes advantage of this by allowing combustion to occur anywhere in the gray-shaded region, while trying to insure that most of the fuel is mixed to $\phi \leqslant 1$ (i.e. the HCCI region) before the reactions are quenched by the expansion, so that good combustion efficiency is maintained. Thus, although diesel LTC combustion is not fully premixed, it uses essentially the same principles as HCCI to obtain low emissions.

Current research and development efforts for advanced CI engines are directed at overcoming the difficulties of implementing HCCI and diesel LTC in practical engines. This requires an improved understanding of the in-cylinder processes for these advanced combustion modes. This article provides an overview of recent research in this area in two parts. In the first part, the technical hurdles for HCCI and partially stratified HCCI engines are discussed along with recent research on the in-cylinder processes directed at overcoming these hurdles. The second part discusses methods for obtaining acceptable diesel-LTC operation and some results of recent investigations of the in-cylinder processes using laser-based imaging diagnostics.

2. HCCI combustion

In principle, HCCI is an ideal combustion process for internal-combustion engines, since it can deliver high thermal efficiencies, comparable with those of conventional diesel engines, and extremely low NO_X and PM emissions [4]. However, HCCI works well only over a relatively narrow operating range, unless engine geometry or operational parameters are adjusted. More specifically, there are four main technical hurdles that must be resolved before HCCI can be applied to practical transportation engines:

(1) improved low-load combustion efficiency,
(2) extension of the operating map to higher loads,
(3) understanding fuel-composition effects on operating limits and design criteria,
(4) control of combustion-phasing over the load/speed range and through transients.

HCCI research and development efforts are focused on overcoming these hurdles. The remainder of this section provides an overview of this work as related to understanding the in-cylinder processes. As such, it will focus mainly on the first two hurdles, with some discussion of fuel effects. Although combustion-phasing control is a critical aspect of HCCI engine development, a discussion is beyond the scope of this article. However, a few comments will be made in the concluding remarks.

2.1. Low-load combustion efficiency

For HCCI engines, the power output is controlled by the fueling rate. Ideally, this is done without throttling in order to maintain high thermal efficiencies. Therefore, as the load is reduced, either the mixture becomes leaner or the amount of dilution with EGR must be increased. Figure 3 shows a plot of the emissions and combustion efficiency for an HCCI engine as a function of ϕ for fully premixed operation with no EGR [19]. The emissions are given as the percentage of total fuel carbon in each exhaust species, to remove changes due solely to the amount of fuel supplied. The engine speed was 1200 rpm, and the 50% burn point (CA50) was held constant at top dead center (TDC) since variations in combustion timing can themselves affect emissions. As can be seen, for moderate loads, $\phi \geqslant 0.2$, carbon monoxide (CO) and hydrocarbon (HC) emissions are low and combustion efficiency is high. However, as ϕ is reduced below 0.2, CO emissions rise dramatically, and the combustion efficiency falls. HC emissions also increase, but to a lesser extent.

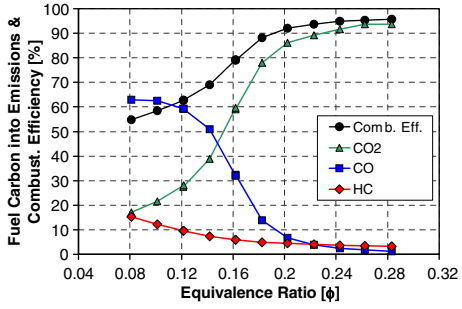

Fig. 3. Combustion efficiency and emissions vs. ϕ for well premixed *iso*-octane and air. 1200 rpm; $P_{in} = 135$ kPa, CR = 14. Adapted from [19].

[1] Unfortunately, these catalysts do not work on diesel or stratified lean-burn SI engines due to excess air in the exhaust.

For a typical idle fueling rate of $\phi = 0.12$ (for complete combustion) or lower, approximately 60% of the fuel carbon remains as CO in the exhaust, HC emissions rise to 10% or more, and combustion efficiencies fall to 62% or less. The reason is that at these low loads, the mixtures are so dilute that combustion temperatures are too low (typically below 1500 K) for the bulk-gas reactions (particularly the CO-to-CO_2 reactions) to go to completion before they are quenched by the expansion stroke [20,21].

Although the high CO and HC emissions at these low loads could potentially be controlled with an oxidation catalyst, the low combustion efficiency is a more serious problem. One solution would be to throttle the engine and operate at a higher ϕ, but this would result in a loss of cycle efficiency due to throttling losses. In contrast, charge stratification offers the potential for overcoming this problem without an efficiency penalty. With this technique, the fuel is injected directly into the cylinder sufficiently late so that it does not mix completely with the air before combustion. Thus, the mixture is locally richer, so it burns hotter, significantly increasing combustion efficiency [19,20,22,23]. Figure 4 presents a demonstration of this technique. Shown are plots of the emissions and combustion efficiency for $\phi = 0.12$ as the injection timing is swept from 20° CA (crank angle) after TDC (aTDC) intake to 325° CA, which is well up the compression stroke. As fuel-injection timing is delayed, the CO emissions fall, slowly at first and then more rapidly for start of injection (SOI) beyond 240° CA. The corresponding sequence of quantitative "ϕ-map" images in Fig. 5 shows how the delayed injection affects the fuel distribution, producing locally higher equivalence ratios that burn hotter and more completely. These images were obtained in an optically accessible engine that closely matches the geometry of the engine used for the data in Figs. 3 and 4 [19]. A schematic of the engine showing the laser-sheet and camera orientation is given in Fig. 6.

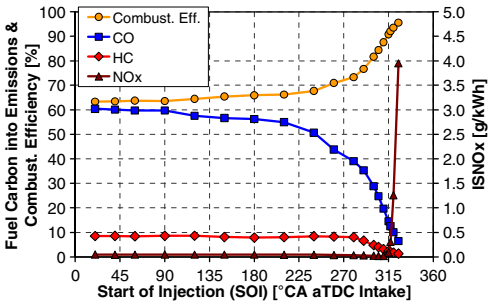

Fig. 4. The effect of varying SOI on combustion efficiency and emissions, using an 8-hole gasoline direct injector with *iso*-octane fuel. 1200 rpm; $\phi = 0.12$; CR = 14; $P_{in} = 135$ kPa; $P_{inj} = 120$ bar; intake temperatures were set so CA50 = TDC, from [19].

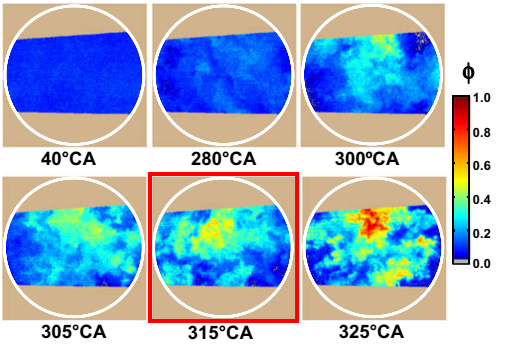

Fig. 5. Series of ϕ-maps of the fuel distribution as SOI is delayed, derived from PLIF images acquired at 365° CA in the mid-plane of the combustion chamber. Conditions are the same as for Fig. 4. The 315° CA image corresponds to the knee in the NO_X curve in Fig. 4. Adapted from [19].

At later SOIs, HC emissions fall as well. Recent research has shown that this is due in large part to fuel no longer having time to reach the top ring-land and head-gasket crevices and the colder region near the cylinder wall [24], although the creation of regions with a higher local ϕ that burn more completely also contributes to this reduction. This finding is in agreement with earlier work showing that the top ring-land crevice was a major source of HC emission in HCCI engines [25]. With the reduction in CO and HC, the combustion efficiency rises substantially, producing a higher gross indicated mean effective pressure ($IMEP_g$). However, if the SOI is delayed beyond 315° CA, NO_X emissions begin to rise rapidly. The images in Fig. 5 show that this coincides with

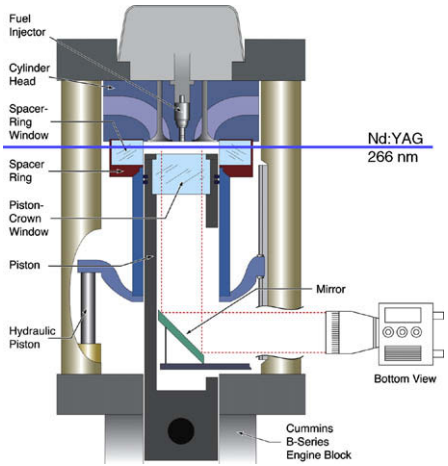

Fig. 6. Schematic of optically accessible HCCI engine.

the stratification producing local regions with $\phi > 0.6$, conditions for which computations indicate that NO_X production will become significant at these operating conditions [19].[2] Thus, the combustion efficiency improvement that can be achieved with fuel stratification is limited by NO_X production. Nevertheless, for the data presented in Fig. 4, stratification improved the combustion efficiency from 62% for premixed fueling to 91% for an SOI of 315° CA, while maintaining near-zero NO_X emissions. With a higher injection pressure, a combustion efficiency of 92.5% was obtained at the US-2010 NO_X limit of 0.27 g/kW h [19].

2.2. High-load limits

High-load HCCI is typically limited by an excessive rate of pressure rise during combustion and the resulting engine knock. This phenomenon is illustrated in Fig. 7a, which shows a series of cylinder-pressure curves for various fueling rates in an HCCI engine, with CA50 held constant at TDC [26]. At a fairly low load, corresponding to $\phi = 0.18$, the pressure-rise rate (PRR) associated with combustion is very moderate. However, the maximum PRR increases substantially as fueling is progressively increased to $\phi = 0.3$. Eventually, the PRR becomes so rapid that it excites an acoustic resonance causing the engine to knock. This creates a distinct ripple on the pressure trace, as evident in the $\phi = 0.3$ curve. Because knocking can cause excessive noise and can lead to engine damage, the maximum PRR must be kept to an acceptable level.

The maximum allowable PRR depends on the engine type and operating conditions such as engine speed and boost pressure [27]. For the data in Fig. 7a, a limit of 9 bar/° CA was subjectively selected based on the perceived noise level. As shown in Fig. 7b, this limit results in a maximum allowable fueling rate of $\phi = 0.27$ for TDC combustion phasing, in agreement with the magnitude of the ripple on the pressure traces in Fig. 7a.

Although the PRR increases substantially with increasing ϕ, it does not increase nearly as rapidly as it would if the charge were fully homogeneous. In a real engine, however, it is not possible to produce a charge that is fully homogeneous in both mixture and temperature, so a single-zone CHEMKIN (Senkin application) computation was used for the comparison in Fig. 7a. For the homogeneous charge, the increase in PRR with ϕ is much more rapid than observed experimentally and knocking becomes unacceptable for $\phi > 0.18$ (Fig. 7b).

[2] The exact ϕ at which NO_X production becomes significant will vary with engine operating parameters and fuel type.

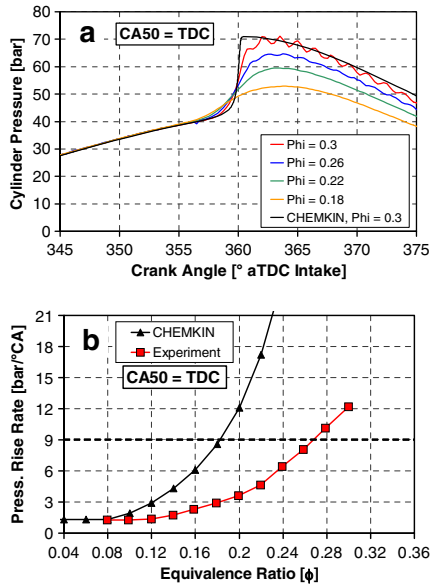

Fig. 7. Experimental cylinder-pressure traces as compared to a homogeneous charge simulated with CHEMKIN (a). Maximum PRR for the experiment and a homogeneous charge (CHEMKIN simulation), (b). Reproduced from [26].

The reduced PRR of the real engine, and the corresponding increase in allowable ϕ, is due to naturally occurring thermal stratification. As shown in Ref. [26], this thermal stratification is caused by wall heat transfer and turbulent mixing during the compression stroke for a low-residual engine such as the one used for the data in Fig. 7. For engines with high levels of retained residuals, incomplete mixing between the fresh charge and hot residuals could also contribute to the thermal stratification [28]. As a result of thermal stratification, combustion does not occur simultaneously in all parts of the chamber, as evident in the chemiluminescence images presented in Fig. 8a. Rather, combustion occurs sequentially beginning with the hottest zone, followed by the next hottest, and so on. This sequential autoignition has been verified experimentally by high-speed image sequences of both natural chemiluminescence [26] and fuel distributions [29]. The sequential autoignition slows the PRR considerably, allowing the fueling to be increased from $\phi = 0.18$ to 0.27 for the TDC combustion-phasing shown in Fig. 7b.

2.2.1. Understanding thermal stratification

Since heat transfer occurs at the walls, thermal boundary layers are often considered to play a major role in the thermal stratification in HCCI engines. However, recent research based on chemiluminescence imaging [26,30] and fuel-tracer PLIF imaging [30] has shown that thermal strati-

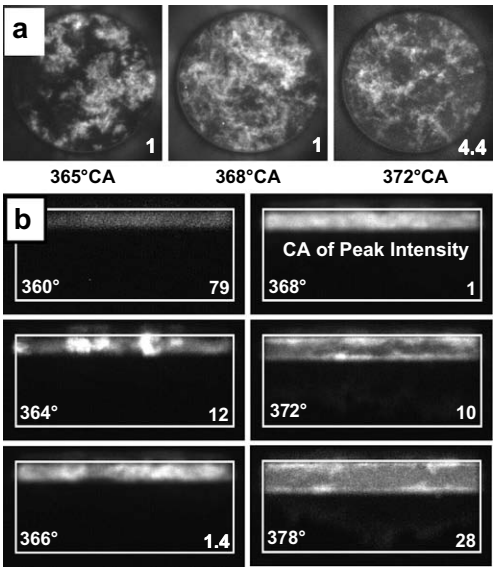

Fig. 8. Chemiluminescence images sequences of HCCI combustion obtained through the piston-crown (a), and spacer-ring (b) windows, see Fig. 6. *Iso*-octane, 1200 rpm, $\phi = 0.38$, CA50 = 368° CA. Relative intensifier gains are given at the lower right of each image. Adapted from [26].

fication extends throughout the bulk gas. This is indicated by the images in Fig. 8a, and it is even more evident in the side-view chemiluminescence image sequence in Fig. 8b [26]. These images were acquired through one of the spacer-ring windows at the top of the cylinder wall (see Fig. 6) with CA50 = 368° CA. As evident in the 364° CA image, hot ignition begins in localized regions in the central part of the charge. From 364–368° CA, the number of regions showing hot ignition increases rapidly although inhomogeneities remain (Fig. 8a). Up past the time of the peak heat-release rate (368° CA), hot ignition and combustion occur in the central part of the charge, i.e. the bulk gases [26]. There is no indication of any preferential boundary-layer combustion until 370° CA. Then, by 372° CA, the boundary layer combustion along the firedeck and piston-top surfaces becomes even more distinct, while the chemiluminescence in the central region dies out.[3] Since the vast majority of combustion occurs in the central part (in the vertical direction) of the charge up past the time of the maximum PRR (367.75° CA), it is mainly thermal stratification within the bulk gases that controls the maximum PRR and engine knock. The effect of thermal stratification between the bulk gases and the boundary layer has only a secondary effect on reducing the maximum PRR. A more complete discussion may be found in Ref. [26].

Since the maximum PRR is controlled by the amount of thermal stratification, researchers have explored various methods of increasing the thermal stratification with the goal of extending the high-load limit of HCCI. However, the results discussed in the previous paragraph show that these techniques must affect the temperature distribution in the bulk gases to be effective for reducing the PRR. This may explain why techniques such as reducing the wall temperature (by lower coolant temperatures) [31,32] have met with only limited success. Other methods of increasing the thermal stratification have also been attempted such as, combining swirl with a square piston bowl [33], and using different intake-air temperatures in each intake port [34,35]. In addition, incomplete mixing of fresh charge with hot retained residuals has also been suggested as a method of increasing the thermal stratification [28,36]. These techniques have shown promise, and research efforts continue, but significant enhancement of the naturally occurring thermal stratification remains a challenge.

2.2.2. Combustion-phasing retard

Despite this limited success at increasing the thermal stratification, substantially higher fueling rates than the $\phi = 0.3$ condition shown in Fig. 7 can be achieved without knock by retarding the combustion-phasing. Up to certain limits, this technique is very effective for slowing the maximum PRR [5,31,37], and it was used while obtaining the images in Fig. 8, for which $\phi = 0.38$ and CA50 = 368° CA. The effect of combustion-phasing retard on the maximum PRR is more clearly evident in the data from the all-metal (non-optical) engine presented in Fig. 9 [38]. In this figure, the smooth curves are the experimental data (the stair-step curves will be discussed below). As can be seen, the rate of pressure rise is reduced substantially (from 14 bar/° CA to 4.7 bar/° CA) as

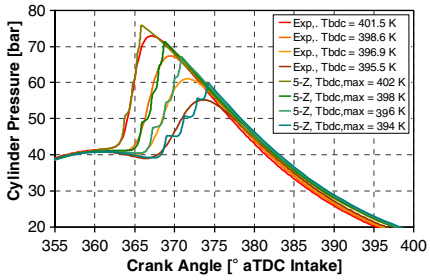

Fig. 9. Combustion-phasing sweeps for the experiment and model. *Iso*-octane, 1200 rpm, $\phi = 0.38$. Reproduced from [38].

[3] At this operating condition the chemiluminescence has been shown to track the heat-release rate well during the main hot combustion period [26].

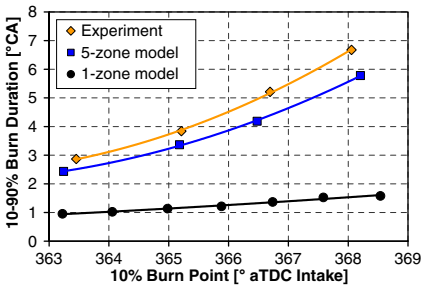

Fig. 10. 10–90% burn duration vs. 10% burn point for the experiment and 5-zone model results in Fig. 9. Single-zone model results also shown. Reproduced from [38].

CA50 is retarded from 365 to 371° CA. This reduction in PRR would allow the fueling rate to be increased without knock.

Analysis of the pressure curves in Fig. 9 shows that the reduced PRR is related to an increase in burn duration with combustion-phasing retard, as shown by the top curve in Fig. 10 [38].[4] Since retarded combustion-phasing results in lower combustion temperatures, it has been considered that this would slow the kinetic rates of the combustion reactions, thereby increasing the burn duration. However, single-zone chemical-kinetic modeling, which accounts for this effect, shows only a modest increase in burn duration with timing retard, as shown by the bottom curve in Fig. 10.

These findings suggest that the thermal stratification, which is not captured in the single-zone model, might play an important role. To investigate this, a multi-zone chemical-kinetic model was applied to account for the effects of having different temperature regions within the charge [38]. The model was configured with only five zones to save computational time – four combusting zones and one non-combusting zone that accounts for boundary-layer and/or crevice regions that do not burn completely. The four active zones were of equal mass and equal thermal width (TW). The total TW of the four zones at bottom dead center (BDC) was then adjusted so the average PRR matched that of the experiment for a base condition, simulating the effect of natural thermal stratification. Then, using this fixed $TW_{bdc} = 20$ K, T_{bdc} was varied so that CA50 matched that of the experimental data for the four combustion-phasings shown. The computed pressure traces shown in Fig. 9 have a stair-step appearance due to the limited number of zones, but it can be seen that the changes in the overall PRR with combustion-phasing closely match the changes in the experimental curves. This is more clearly evident in Fig. 10, which shows very similar changes in burn duration for the multi-zone model (middle curve) and the experiment (top curve).[5] In addition, the required changes in T_{bdc} match very closely to those required for the experimental data, as shown in the legend.

The reason that thermal stratification increases the reduction in PRR with combustion-phasing retard is related to the volume-expansion. With a thermally stratified charge, combustion occurs first in the hottest zone. This combustion then further compresses the remaining charge increasing its temperature and pressure. After an induction time, the next hottest zone autoignites, and the process repeats, as evident in the pressure traces for the multi-zone model in Fig. 9. When combustion occurs after TDC, the expansion increases the induction time, slowing the sequential autoignition of each successively cooler zone. With greater combustion-phasing retard, the rate of expansion due to piston motion increases, further delaying the autoignition of successively cooler zones and slowing the overall PRR. Thus, the main reason combustion phasing retard reduces the PRR in HCCI engines is that it amplifies the effect of the thermal stratification. This is discussed in greater detail in Refs. [38,40].

2.2.3. Phasing-retard limits

Although combustion-phasing retard is very effective for slowing the PRR to allow higher loads, the amount of allowable retard is limited by poor cycle-to-cycle stability and eventually misfire [31,41]. As the combustion-phasing is retarded beyond about 370–375° CA (10–15° aTDC) (depending on operating conditions), the standard deviation of the autoignition timing as measured by the 10% burn point (CA10) begins to increase significantly. These variations are thought to result from small variations in the bulk-gas temperature produced by turbulence effects on the convective heat transfer. With retarded combustion-phasing, the more rapid piston expansion causes these small temperature variations to have a larger effect on CA10. In turn, these variations in CA10 affect the burn duration, leading to partial misfire when the burn duration becomes so long that expansion quenches the combustion in the coldest zones [31,38]. The net effect is increased variations in the $IMEP_g$ as well

[4] The greater volume and greater volume-expansion rate with combustion-phasing retard will contribute to the reduced PRR independently of changes in the heat-release rate [39], but to a lesser degree than changes in burn duration [7].

[5] The slightly greater change in burn duration for the experiment is thought to result from an increase in thermal stratification during the combustion event due to on-going convective heat transfer, as discussed in Refs. [31,38].

as CA10, and eventually complete misfire as the phasing becomes overly retarded.

As a result, the combustion-phasing must be maintained between the knocking and stability/misfire limits. This becomes increasing difficult as the fueling is increased because the spread between these limits narrows, and because it often becomes more difficult to control the combustion-phasing at high loads [31,37], as will be discussed in the next sub-section. In addition, when fueling is increased sufficiently, it is also possible to produce NO_X emissions that exceed US-2010 limits.

For these reasons, practical HCCI engine operation is currently limited to about half of the load that is typical for SI or diesel engine operation. As a result, engine manufacturers are developing strategies for hybrid-combustion systems in which the engine operates in HCCI mode at low loads and reverts to SI or diesel operation at high loads. In automotive applications, most operation is at half load or less, so significant fuel-economy benefits are still realized. For diesel engines, part-load HCCI or LTC could significantly reduce the expense and/or service intervals of an aftertreatment system. However, because it is advantageous to extend HCCI operation over as much of the driving cycle as possible, and because there are clear advantages to a full-time HCCI engine, extending the high-load limit of HCCI operation is an area of active research.

2.3. Fuel effects

Although many fuels have been used in HCCI/LTC engines, most research efforts for transportation engines have focused on gasoline or diesel fuel. Gasoline and *iso*-octane (a good gasoline surrogate [42,43]) are some of the most commonly used fuels for HCCI research, including the data presented above in Sections 2.1 and 2.2. Their relatively high volatility is advantageous for mixture formation, and there is a strong interest in using gasoline-like fuels for HCCI due to their availability and their application to HCCI/SI hybrid-combustion systems. Under typical non-boosted HCCI operating conditions, these fuels exhibit only a single-stage autoignition, which requires a relatively high autoignition temperature.[6]

[6] Although all commercial gasolines require relatively high temperatures for non-boosted conditions, differences in gasoline composition can affect autoignition and performance in HCCI engines. Since standard octane numbers do not adequately rank fuels for HCCI, Kalghatgi and co-workers [44,45] have suggested the use of an octane index, which is deduced from the RON and MON with an empirical constant for engine operating conditions. Another approach that has shown potential is the development of an HCCI ignition index based on the fuel composition [46].

In contrast, mixture formation is more difficult with diesel fuel due to its low volatility, and diesel fuel has a strong two-stage ignition process making it difficult to prevent early autoignition when it is premixed. As a result, diesel-fueled HCCI-like combustion is typically accomplished in a different manner, as discussed in Section 3. Although these traditional fuels are more commonly used, research has shown that there may be advantages to operating with fuels that have ignition characteristics which are intermediate between these two [12,47–49]. In particular, fuels that exhibit some two-stage autoignition, but less than that of diesel fuel, appear to have significant advantages [7,49]. It is also advantageous if these fuels are sufficiently volatile for well-controlled mixture formation.

Figure 11 shows a comparison of the cylinder-pressure and mass-averaged temperature for *iso*-octane and PRF80 (a mixture of the gasoline primary reference fuels consisting of 80% *iso*-octane and 20% *n*-heptane) [41]. As can be seen, PRF80 has low-temperature heat-release (LTHR) beginning at about 340° CA, which increases its temperature and pressure prior to the main hot ignition at about 367° CA (two-stage ignition). In contrast, *iso*-octane shows no significant heat-release until the hot ignition at about 367° CA (single-stage ignition). Because of the LTHR, PRF80 requires a much lower intake temperature than *iso*-octane for the same CA50, as reflected by the lower temperature at the far left of the plot in Fig. 11 (260° CA). This lower temperature is advantageous because it means that the intake-charge density is higher, so more charge mass is inducted into the cylinder. Therefore, PRF80 gives a significantly higher power output for the same charge-mass/fuel (C/F) ratio.

Another advantage of a fuel with some LTHR is that it has a higher heat-release rate prior to the main hot ignition. This can be seen by a comparison of the temperature traces in Fig. 11 (see

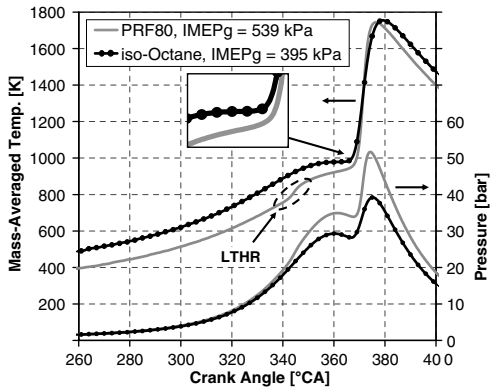

Fig. 11. Temperature and pressure traces for *iso*-octane and PRF80 ($\phi = 0.40$), from [41].

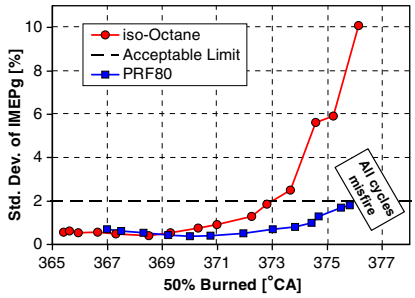

Fig. 12. Standard deviation of $IMEP_g$ divided by ($IMEP_g - IMEP_{g,motored}$) as a function of CA50, from [41].

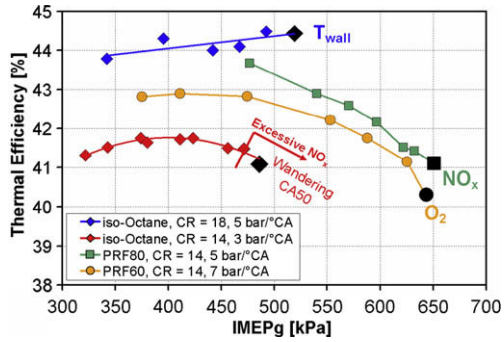

Fig. 13. Thermal efficiency vs. $IMEP_g$ for *iso*-octane, PRF80, and PRF60. The load-limiting factor is indicated for each curve as explained in the text, from [7].

inset). For *iso*-octane, the temperature increases only slightly for the 10° CA prior to hot ignition, whereas for PRF80 there is a strong upward slope to the temperature curve. This occurs because the LTHR enhances the intermediate-temperature chemistry leading up to hot ignition [50]. Having a higher rate of temperature-rise prior to hot ignition reduces the cycle-to-cycle variations in autoignition phasing (CA10) associated with small random charge-temperature variations [41]. Additionally, the LTHR tends to dampen out random temperature variations because lower temperatures lead to increased LTHR, which increases the temperature prior to hot ignition, and vice versa. These compensating changes in LTHR reduce magnitude of the random temperature variations prior to hot ignition [41]. As a result of the greater temperature-rise rate prior to hot ignition, and the reduced magnitude of cycle-to-cycle temperature fluctuations, PRF80 can tolerate a greater combustion-phasing retard while maintaining an acceptable standard deviation of the $IMEP_g$, as shown in Fig. 12 and Ref. [49].

With the combination of greater allowable timing retard and a greater inducted charge mass, significantly higher loads have been achieved under naturally aspirated conditions by using a fuel that has some two-stage ignition [7]. Figure 13 shows the highest loads ($IMEP_g$) and thermal efficiencies achieved in Ref. [7] for *iso*-octane, PRF80, and PRF60 (60% *iso*-octane, 40% *n*-heptane).[7] All data are for a compression ratio (CR) of 14, except the upper *iso*-octane dataset, which was taken with CR = 18. As can be seen, a maximum $IMEP_g$ of about 650 kPa was reached for PRF80 and PRF60, while for *iso*-octane, the load was limited to an $IMEP_g$ of 486 or 520 kPa for CR = 14 or 18, respectively. The reduced thermal efficiency with increasing load for PRF60 and PRF80 is due to the increased combustion-phasing retard required to maintain an acceptable PRR. It is also noteworthy that increasing the CR to 18 for *iso*-octane increased the thermal efficiency and allowed a higher $IMEP_g$ compared to CR = 14.

The mechanism limiting the maximum load varies with fuel type, as noted in Fig. 13. For *iso*-octane, the high-load limit results from the high sensitivity of combustion-phasing to small changes in the charge temperature. As a result, small changes in the wall temperature can cause CA50 to advance to runaway knock or retard to misfire, as occurs for the CR = 18 case [31]. In other cases, this high sensitivity causes an inability to adequately control combustion-phasing (i.e. wandering CA50), as occurs for the CR = 14 case with a PRR = 3 bar/° CA. Similar temperature sensitivity was noted by Olsson et al. [37] who demonstrated that it is possible to operate at higher loads if a fast closed-loop control system was implemented to maintain combustion phasing.

PRF fuels with LTHR are less sensitive to changes in temperature and are load-limited by other factors. For PRF80, the load can be increased until the combustion becomes sufficiently hot to produce small amounts of NO_X. Although emissions are still well below the US-2010 limits, very low concentrations of NO_X (a few ppm) transferred to the incoming charge through the residuals or EGR enhance the autoignition [7,51], rapidly advancing the combustion-phasing to runaway knock [7]. A fast closed-loop control system might also extend this limit depending on the NO_X-feedback timescales. Finally, for PRF60 at the conditions studied, the high load was limited by the available oxygen. This is because the greater LTHR with PRF60 requires that substantial amounts of EGR be used to retard the combustion-phasing to maintain an acceptable PRR. Alternatively, a lower compres-

[7] Intake-pressure boosting offers the potential for even higher loads for both single- and two-stage fuels. Research in this area has involved a variety of fuels, with the highest loads obtained using natural gas combined with a small amount of *iso*-octane [6,9].

sion ratio would reduce the required EGR and likely allow a higher $IMEP_g$, but at the expense of a further reduction in the thermal efficiency.

Although PRF60 is the most reactive fuel used in Ref. [7], with a computed cetane number of 30, it has significantly less LTHR than typical diesel fuels, which have cetane numbers ranging from 45 to 55. Because of this increased reactivity, preventing the combustion-phasing from becoming overly advanced with diesel fuel is challenging, as discussed in the following section.

3. Diesel LTC combustion

Conventional CI diesel combustion gives high fuel-efficiency, but further reductions in NO_X and soot emissions are required. Because of HCCI's potential to reduce these emissions while maintaining high efficiency, there has been considerable interest in applying HCCI or HCCI-like low-temperature combustion to diesel engines. However, achieving acceptable HCCI combustion with diesel fuel is complicated by its low volatility and high cetane number. Although in principle, other fuels could be used, there are several reasons why diesel-fueled operation is desirable, such as offering the ability to revert to more-conventional diesel operation at high loads, as discussed in Ref. [4].

Initial attempts to obtain diesel-fueled HCCI involved premixing using intake-port fuel-injection [8,13,14]. However, significant intake heating (135–205 °C) was required to minimize the accumulation of liquid fuel in the intake system and to prevent soot and NO_X formation as a result of in-cylinder inhomogeneities. This heating, combined with the high cetane number of diesel fuel, required that the CR be reduced, typically to values in the range of 9–11 to prevent knocking. In addition, combustion efficiency was poor due to high levels of unburned HC. As a result of the reduced CR and incomplete combustion, fuel consumption increased significantly compared to conventional diesel combustion, although NO_X and smoke levels were substantially reduced.

3.1. Very early direct-injection LTC

To overcome the vaporization and mixing issues, later works investigated early direct injection (DI) fueling [4] as a way to obtain near-HCCI combustion. By injecting part way up the compression stoke, the higher in-cylinder temperatures and densities promote vaporization and mixing. However, obtaining good mixing in the reduced time available and preventing wall wetting due to spray over-penetration can be challenging. Various fuel-injector types and techniques have been investigated, and in general, injectors producing a softer, more-disperse spray have produced better results for early injection schemes [15,47,52]. However, more-conventional DI diesel injectors have the advantage of allowing a switch to conventional diesel combustion at high loads. They also allow dual-injection schemes [52–54], in which part of the fuel is injected early and part at a conventional diesel timing near TDC (e.g., the Toyota "UNIBUS" system [52]). Unfortunately, liquid-spray impingement on the cylinder liner often occurs when a conventional diesel injector is used for very early injection. One interesting approach for overcoming this problem is to direct the fuel sprays more steeply downward (narrow included angle) so they are still directed at the piston bowl for early injection, as described by Walter et al. [55]. An injection system combining a soft spray for early injection with a conventional diesel injector for late injection has also shown promise [56,57].

Even with the improved mixture formation of these early-DI systems, the high cetane number of diesel fuel can lead to early ignition and knocking. Therefore, nearly all approaches use high levels of cooled EGR to slow the autoignition process [47,55,58]. Additionally, somewhat reduced compression ratios of 14:1 or 15:1 are often employed in the diesel-HCCI concepts [55,59], and some approaches also use late intake valve closing (IVC) to further reduce the effective compression ratio [57,60,61]. Late IVC has the advantage of allowing the effective compression ratio be rapidly adjusted as part of the control system, and a high expansion ratio is preserved for good cycle efficiency. Even with these controls, maintaining the desired combustion-phasing with changes in speed and load remains a challenge for these early injection techniques in which the autoignition timing is only controlled by the chemical kinetics. High HC emissions have also been reported [59]. However, early-injection approaches continue to be an area of research, and they are sometimes considered as part of an overall combustion strategy [57,59].

3.2. Near-TDC direct-injection LTC

A second approach to low-temperature diesel combustion is to inject the fuel closer to TDC, so that combustion is more closely coupled to the injection event [18,59,62]. In this manner, the combustion-phasing can be controlled somewhat independently from the autoignition kinetics of the fuel. Since injection occurs near TDC, high-pressure injectors are required for rapid mixing, and various techniques must be applied to extend the ignition delay to allow more time for premixing in order to obtain LTC and the associated low emissions. One relatively common technique for extending the ignition delay is to retard injection so that the jet-mixing process occurs in the early part of the expansion stoke, slowing the autoignition. This concept was first introduced under the

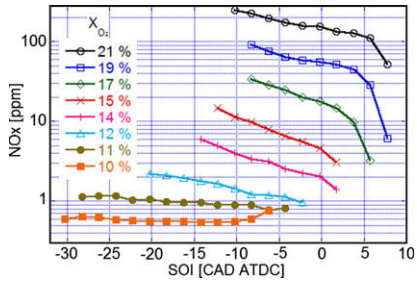

Fig. 14. NO_X emissions as a function of SOI for diesel LTC with various EGR levels (given as O_2 concentration). The engine was skipfired, so true emissions are four times the values shown. Adapted from [18].

name of MK (modulated kinetics) combustion [63]. It is also possible to extend the ignition delay by injecting earlier than conventional diesel (20–30° bTDC), but not so early that the autoignition becomes decoupled from the injection event. However, with this approach, it can be difficult to prevent combustion from occurring before TDC, which often increases noise and reduces engine efficiency. In addition to late (or early) injection timing, techniques such as high levels of cooled EGR, reduced CR, and/or late IVC are often applied to increase the ignition delay, similar to the early-injection, chemical-kinetically controlled approach discussed above.

Even with very rapid mixing and increased ignition delay, it is difficult to produce a well-mixed dilute charge at the time of autoignition, and a significant fraction of the heat is released in a mixing-controlled process [18]. Accordingly, high levels of EGR are required to keep local peak-combustion temperatures sufficiently low to prevent NO_X formation, in addition to their benefit for increasing ignition delay.

This second diesel LTC approach has been demonstrated both for injection timings earlier and later than conventional diesel [17,62–64]. To clarify the trade-offs between early and late injection, and the effects of EGR, Kook et al. [18] recently conducted an investigation over a wide range of EGR levels and injection timings. This study used an automotive-sized single-cylinder research diesel engine (0.42 l) at a 3 bar IMEP operating condition. Figure 14 shows the NO_X emissions over this range of conditions. As can be seen, for low levels of EGR (high O_2 concentrations), NO_X is high unless injection timing is retarded so that there is sufficient premixing for a significant portion of the fuel to burn under lower-temperature conditions.[8] Temperatures are

[8] For low EGR levels, there are no data earlier than those shown in Fig. 14 because data were not acquired for injection timings causing a fuel consumption penalty of more than 10% [18].

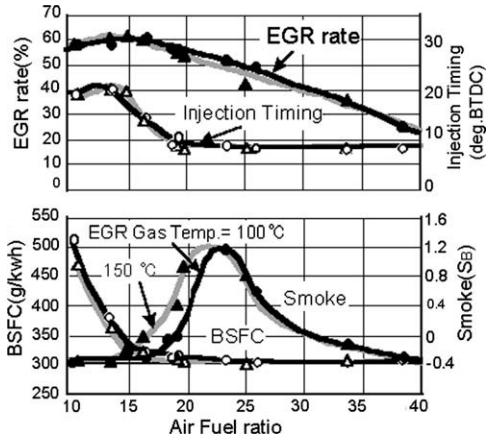

Fig. 15. Smoke emissions as a function of EGR, plotted in terms of A/F for a constant IMEP = 0.2 MPa. Two different EGR temperatures are shown. Adapted from [17].

also reduced because there has been some charge expansion before combustion occurs, and there is less time available before the NO_X-producing reactions are quenched by the expansion. (Note that combustion occurs well after the SOIs shown.) However, for zero or low levels of EGR, NO_X emissions are generally still too high to meet the US-2010 standards even with retarded injection timing. As EGR levels increase (reduced O_2 concentrations), NO_X emissions fall substantially, and the additional NO_X reduction with highly retarded injection becomes less. At the highest EGR levels, combustion temperatures are sufficiently low that NO_X emissions remain very low for all injection timings.

Understanding trends in soot emissions with this second LTC approach is more complex because they are the result of a competition between soot formation and oxidation processes. Increasing the amount of premixing by early or late injection timing decreases the total soot luminosity, suggesting that soot formation is reduced as might be expected [18,64]. EGR addition, however, first increases then decreases soot emissions (smoke) as shown in Fig. 15 [17]. The substantial increase in smoke as the air/fuel ratio (A/F) is reduced from 40 to 23 (at constant IMEP = 0.2 MPa) is thought to be mainly the result of reduced soot oxidation due to the lower oxygen concentration and lower combustion temperatures. EGR can also increase soot residence times in the reacting fuel jet, causing increased soot formation for moderate EGR levels [65]. In contrast, reducing the A/F below 23 by adding more EGR reduces the smoke (Fig. 15). This occurs because combustion temperatures in fuel-rich regions are reduced to the point that soot formation is suppressed to a greater degree than soot oxidation [17]. This is most easily understood by examination

of Fig. 2. Soot formation in diesel engines typically occurs for $2 \leqslant \phi \leqslant 4$. For zero EGR, combustion temperatures are near the adiabatic flame-temperature line shown, which is well into the soot formation region. As EGR is added, combustion temperatures are reduced, shifting the rich-combustion conditions to the left, away from the soot-formation region. With sufficient EGR, smoke levels become very low, but there is only a narrow operating window before fuel consumption (BSFC) rises dramatically (Fig. 15).

As demonstrated by the above data, NO_X and soot can be substantially reduced with this near-TDC injection LTC approach. Moreover, this technique still provides good control of the combustion phasing by adjusting the injection timing. However, Refs. [17,18] report significantly increased CO levels for their high EGR conditions. Also, HC emissions are typically reported to be much higher than those of conventional diesel combustion [59,66], but still less than those for the very early injection diesel LTC discussed in Section 3.1.

3.3. Imaging of near-TDC direct-injection LTC combustion

As discussed above, obtaining low NO_X and PM emission with near-TDC injection LTC requires high levels of dilution with EGR and shifting the injection timing 10–15° CA earlier or later than for conventional diesel combustion to create a long ignition delay and significant premixing. To better understand how this type of LTC occurs, advanced laser-sheet and natural-luminosity imaging diagnostics have been applied [64–71]. Imaging of LTC combustion has also helped identify the sources of increased HC [66,71] and CO emissions [71].

Figure 16 shows a series of simultaneous images of natural chemiluminescence and liquid-fuel contours for a low-load LTC condition (IMEP = 4 bar) with an earlier-than-conventional injection-timing of 338° CA (22° bTDC) and 12.7% O_2 in a heavy-duty single-cylinder diesel engine (2.34 l) [72]. Significant chemiluminescence does not appear until about 7.5° after start of injection (ASI) in the region 20–40 mm from the injector. This compares with 4.5° ASI and 15–25 mm for conventional diesel combustion [2]. The images also show that injection has ended, and the liquid fuel has nearly all vaporized before autoignition, as compared to conventional operation where injection continues well into the combustion event [2]. Thus, these images verify that for LTC combustion, the jet penetrates much farther and mixes to substantially more dilute conditions prior to autoignition.

The relatively weak initial chemiluminescence beginning at 7.5° ASI is due to LTHR (first-stage of ignition), and by 10° ASI it occurs

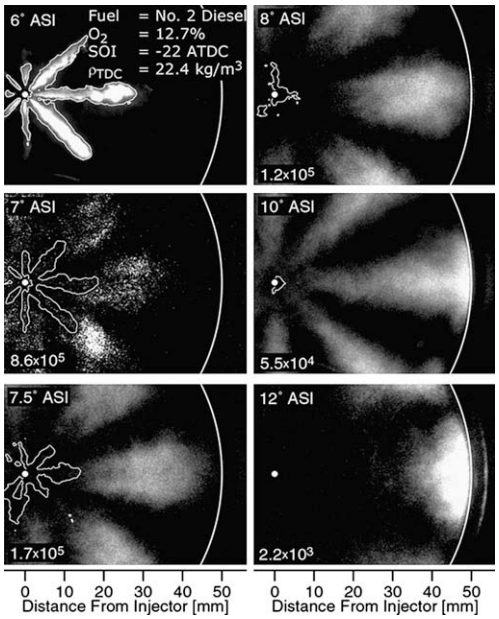

Fig. 16. Sequence of simultaneous images of chemiluminescence and liquid fuel contours for LTC operation. View is upward through the piston-crown window. Adapted from [72].

throughout the jet (Fig. 16). Between 10 and 12° ASI the chemiluminescence becomes much brighter in the region near the piston-bowl wall (note the gain numbers in the lower left of each image). This timing coincides with the onset of the main hot combustion. Note that the increase in chemiluminescence intensity is due not only to the higher heat-release rates associated with the hot combustion, but also to a shift in the source of the chemiluminescence from being mainly formaldehyde emission during the LTHR to arising mainly from the CO-continuum and other radicals such as CH and HCO during the hot combustion [50,73].

In agreement with this shift in the chemiluminescence to the near-wall region, an OH-PLIF signal was detected in this same region beginning at about 14° ASI [72]. A series of simultaneous OH-PLIF and soot luminosity images acquired in the same engine at a similar operating condition (all parameters were the same except for a slightly lower intake pressure, which reduced the TDC density from 22.5 to 16 kg/m^3) are shown in Fig. 17 [64]. These images were acquired through a window in the cylinder head, which provides a close-up view of the downstream region of the fuel jet. The piston bowl-rim has been cut out to allow the jet to penetrate farther before reaching the wall (dashed and solid white curved lines show the edge of bowl and the cylinder wall, respectively). These images show that the hot combus-

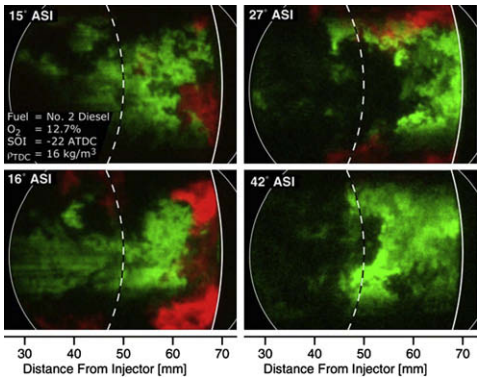

Fig. 17. Simultaneous OH (green) and soot luminosity (red) images for a diesel LTC condition similar to Fig. 15. Adapted from [64].

tion, indicated by the presence of the OH, occurs mainly in the downstream region of the jet. They also show that the OH is broadly distributed throughout the downstream region of the jet, as opposed to forming only in a thin diffusion flame around the jet periphery as in conventional diesel combustion (see Fig. 1) [2]. This broad OH distribution indicates that there are significant regions of the jet that have mixed to stoichiometries near $\phi = 1$, rather than being very fuel-rich ($\phi = 2$–4) like a conventional fuel jet [2,74]. As a result, soot is greatly reduced, but regions of soot luminosity still occur along the wall near the head of the jet, indicating the existence of some fuel-rich regions.

The reduced NO_X and soot emissions, and the broad OH distribution, with LTC indicate that significant premixing has occurred; however, the overall size and shape of the jet are similar to those of conventional diesel jets. This suggests that the total air entrainment for a given jet penetration has not changed significantly, so this cannot be the source of the additional premixing. The main difference in the formation of the LTC jet is that fuel injection ends well before the start of combustion (see Fig. 16 and also [64,72]). With the end of injection, fuel is no longer delivered to the upstream portion of the jet, so the mixture becomes lean much more quickly than for a steady jet, and the combustion occurs in this leaner mixture. More details are given in Ref. [66]. Support for this finding is provided by measurements of the ϕ distribution within a diesel fuel jet during the transient after the end of injection, as shown in Fig. 18. This image was acquired using quantitative Rayleigh-scatter imaging at 5° after the end of injection, which is similar to the timing of the first OH image in Fig. 17. It shows substantial regions near $\phi = 1$ downstream of ~30 mm, the same region where the OH occurs.

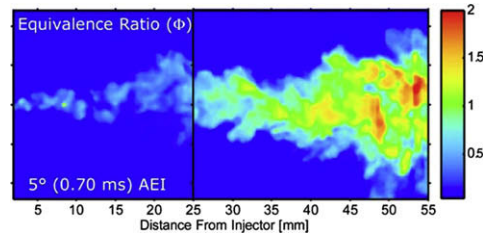

Fig. 18. Rayleigh-scatter ϕ-map image of the diesel fuel jet 5° CA after the end of injection for an LTC condition similar to that of Figs. 15 and 16. Adapted from [66].

Although this improved mixing in the downstream region is central to the benefits of LTC, the image in Fig. 18 also shows that the increased mixing associated with the end of injection causes the upstream region near the injector to become very lean. As discussed in Ref. [66], these overly lean regions are unlikely to burn to completion, and therefore, appear to be a major source for the increased HC emissions with diesel LTC. These high HC emissions combined with the high CO emissions that are often encountered with LTC (see Section 3.2) can lead to poor combustion efficiency and increased BSFC [17,18]. To better understand these issues, a recent imaging study has investigated the sources of CO and HC emissions in a light-duty diesel engine operating under near-TDC injection LTC conditions [71]. This work provides significant insights into the in-cylinder locations where CO and HC arise, the causes of these emissions (both fuel-lean and fuel-rich regions), and how these sources can be affected by operating parameters such as injection timing and increased load.

The results of these imaging studies and other works have considerably advanced our understanding of diesel LTC. However, additional research is required to obtain good combustion efficiency while maintaining low NO_X and soot emissions over a wider operating range. This is particularly important for extending LTC to higher loads since increased fueling and intake boost can reduce the "window" where both low NO_X and high combustion efficiency are obtained (see Fig. 15), and elevated soot levels can extend over this window [75,76].

4. Summary and concluding remarks

Advanced compression-ignition engines have been demonstrated to deliver both high efficiencies and very low NO_X and PM emissions. Like conventional CI diesel engines, relatively high compression ratios and lack of throttling losses provide high efficiencies. However, unlike conventional diesel engines, they operate with highly dilute, premixed or partially premixed combustion

for low emissions. Charge dilution is accomplished either by making the mixture very lean or through the use of high levels of EGR/retained-residuals.

The development of these advanced CI engines has evolved mainly along two lines. First, for fuels other than diesel, a combustion process commonly referred as HCCI is generally used, in which the charge is premixed and then compression ignited. Although the name HCCI indicates a "homogeneous" charge, there are always some thermal inhomogeneities, and in many cases it is desirable to introduce some degree of charge-mixture stratification. With HCCI the fuel/charge distribution are established prior to the final compression to autoignition, which has the advantage of allowing good control over the mixture distribution. HCCI also allows for good air utilization (an advantage for high-load operation), since fuel can be premixed with all the air if desired. With HCCI, the autoignition and combustion-phasing are determined by the chemical kinetics of the prepared mixture. Various techniques have been demonstrated to provide control, such as EGR addition, fast intake-temperature management [77], controlled mixture stratification for two-stage fuels [43,49], variable compression ratio [8] and variable valve timing for residual recompression [28,36,78,79], exhaust rebreathe [28,36,80], or late intake valve closure [60,61].

For diesel fuel, a second approach is commonly used, in which the autoignition is closely coupled to the fuel-injection event. To obtain dilute partially premixed combustion, this approach relies on high levels of EGR. Also, the injection timing is shifted 10–15° CA earlier or later than for conventional diesel combustion so that charge-gas temperatures are reduced, delaying ignition and provide more time for premixing. This approach is referred to here as near-TDC injection LTC although several other acronyms have been used in the literature. This approach provides direct control over the combustion phasing through the injection timing, which helps prevent the overly advanced combustion that can occur with diesel-fueled HCCI. Drawbacks are that fuel and air are not well mixed, so a significant portion of the heat-release can occur as mixing-controlled combustion and care must be taken to maintain low NO_X and PM.

Although the majority of HCCI and LTC research has focused on using existing fuels, other works have shown that fuels with ignition qualities intermediate between gasoline and diesel have potential advantages for extending the operating range of these low-emissions, high-efficiency combustion modes. Also, it should be noted that the two modes are not exclusive to the respective fuel types discussed here. For example, recent research has shown a strong potential for using gasoline-like fuels in a late-injection LTC mode, since their resistance to autoignition provides additional time for premixing [81,82].

5. Future research directions

Over the past decade, substantial progress has been made in understanding the in-cylinder processes in HCCI and diesel-LTC engines, and this has greatly expanded our ability to operate in these combustion modes. Challenges remain, however, and research is needed in several areas.

For HCCI, some of the most important areas are:

- Further improvements in producing stratified mixtures at low loads to obtain good combustion efficiency with low NO_X,
- Methods for enhancing autoignition at low loads for HCCI/SI hybrid-combustion systems,
- Methods for increasing thermal stratification to extend the high-load limit,
- A better understanding of the effects of variations in the composition of gasoline,
- Additional investigations of the effects of changing fuel composition beyond the range of traditional fuels such as gasoline and diesel fuel, and the potential for increasing the HCCI operating range using these alternative fuel mixtures, and
- Improvements in control systems such as those mentioned above in Section 4.

For diesel LTC, an improved understanding is needed in the following areas:

- The sources of CO and HC emissions for LTC strategies with injection both earlier and later than conventional diesel combustion,
- The sources of PM emissions that often occur in the narrow operating window where both low NO_X and good combustion efficiency are achieved,
- Mixture formation and air utilization for fuel-injection strategies using multiple injections, and
- Methods for extending LTC operation to higher loads while maintaining good fuel-economy and low emissions.

In addition, both HCCI and diesel LTC would benefit from:

- Improved jet-mixing models,
- A better understanding of the effects of intake-pressure boost,
- Better predictive capability of in-cylinder flows and turbulence and their effects on fuel/air/EGR-residual mixing and thermal stratification,

- Improved chemical-kinetic models that more accurately predict LTHR, pressure-boost effects, and the behavior of realistic fuels,
- Low-temperature lightoff oxidation catalysts for controlling HC and CO emissions at low loads, and
- Less expensive pressure transducers or other combustion/ignition sensors for closed-loop feedback control.

Acknowledgments

The author would like to express his gratitude to following people from Sandia National Laboratories for valuable discussions and helpful explanations of their work (in alphabetical order): Sanghoon Kook, Paul Miles, Charles Mueller, Mark Musculus, Lyle Pickett, Magnus Sjöberg, and Richard Steeper.

Support was provided by the U.S. Department of Energy, Office of Vehicle Technologies, managed by Gurpreet Singh. Sandia is a multiprogram laboratory operated by the Sandia Corporation, a Lockheed Martin Company, for the United States Department of Energy's National Nuclear Security Administration under contract DE-AC04-94AL85000.

References

[1] EPA emission standards may be found at: http://www.dieselnet.com/standards/.
[2] J.E. Dec, *SAE Trans.* paper 970873 106 (3) (1997), 1319–1348.
[3] J.E. Dec, R.E. Canaan, *SAE Trans.* paper 980147 107 (3) (1998) 176–204.
[4] F. Zhao, F., T.W. Asmus, D.N. Assanis, J.E. Dec., J.A. Eng, P.M. Najt, *Homogeneous Charge Compression Ignition (HCCI) Engines: Key Research and Development Issues*, Society of Automotive Engineers, Warrendale, PA, 2003.
[5] M. Christensen, B. Johansson, B. *SAE Trans.* paper 982454 107 (4) (1998) 951–963.
[6] M. Christensen, B. Johansson, P. Amnéus, F. Mauss, *SAE Trans.* paper 980787 107 (3), 1998.
[7] M. Sjöberg, J.E. Dec, *SAE Trans.* paper 2008-01-0054 117, 2008, in press.
[8] M. Christensen, A. Hultqvist, B. Johansson, *SAE Trans.* paper 1999-01-3679 108 (3), 1999.
[9] M. Christensen, B. Johansson, *SAE* paper 2000-01-1835, 2000.
[10] M. Yao, Z. Chen, Z. Zheng, B. Shang, Y. Xing, *Fuel* 85 (2006) 2046–2056.
[11] P. Risberg, G. Kalghatgi, H.-E. Ångström, F. Wåhlin, *SAE Trans.* paper 2005-01-2127 114 (4) (2005) 883–893.
[12] N. Kaneko, H. Ando, H. Ogawa, N. Miyamoto, *SAE Trans.* paper 2002-01-1743 111 (3) (2002) 2309–2315.
[13] T.W. Ryan III, T.J. Callahan, *SAE Trans.* paper 961160 105 (4), 1996.
[14] A. Gray, T.W. Ryan III, *SAE Trans.* paper 971676 106 (3), 1997.
[15] Y. Iwabuchi, K. Kawai, T. Shoji, Y. Takeda, *SAE Trans.* paper 1999-01-0185 108 (3), 1999.
[16] T. Kamimoto, M.-H. Bae, *SAE Trans.* paper 880423, 97 (3), 1988.
[17] K. Akihama, Y. Takatori, K. Inagaki, S. Sasaki, A.M. Dean, *SAE Trans.* paper 2001-01-0655 110 (3), 2001.
[18] S. Kook, C. Bae, P.C. Miles, D. Choi, L.M. Pickett, *SAE Trans.* paper 2005-01-3837 114 (4), 2005.
[19] W. Hwang, J.E. Dec, M. Sjöberg, *SAE Trans.* paper 2007-01-4130 116 (3), 2007.
[20] J.E. Dec, M. Sjöberg, *SAE Trans.* paper 2003-01-0752 112 (3) (2003) 1119–1141.
[21] M. Sjöberg, J.E. Dec, *Proc. Combst. Inst.* 30 (2005) 2719–2726.
[22] R.R. Steeper, S. De Zilwa, *SAE* paper 2007-01-0180, 2007.
[23] P.W. Aroonsrisopon, P. Werner, J.O. Waldman et al., *SAE Trans.* paper 2004-01-1756 113 (3), 2004.
[24] J.E. Dec, M.L. Davisson, R.N. Leif, M. Sjöberg, W. Hwang, *SAE Trans.* paper 2008-01-0053 117, 2008, in press.
[25] M. Christensen, B. Johansson, A. Hultqvist, *SAE* paper 2001-01-1893, 2001.
[26] J.E. Dec, W. Hwang, M. Sjöberg, *SAE Trans.* paper 2006-01-1518 115 (3) (2006) 759–776.
[27] J.A. Eng, *SAE* paper 2002-01-2859, 2002.
[28] A. Babajimopoulos, G.A. Lavoie, D.N. Assanis, *SAE* paper 2003-01-3220, 2003.
[29] A. Hultqvist, M. Christensen, B. Johansson et al., *SAE Trans.* paper 2002-01-0424 111 (3), 2002.
[30] D.L. Reuss, V. Sick, *SAE Trans.* paper 2005-01-2122 114 (4), 2005.
[31] M. Sjöberg, M., J.E. Dec, A. Babajimopoulos, D.N. Assanis, *SAE Trans.* paper 2004-01-2994 113 (3) (2004) 1557–1575.
[32] J. Chang, Z. Filipi, D. Assanis, T.-W. Kuo, P. Najt, R. Rask, *Int. J. Engine Res.* 6 (2005) 289–309.
[33] M. Christensen, B. Johansson, *SAE* paper 2002-01-2864, 2002.
[34] A. Kakuho, M. Nagamine, Y. Ameromori, T. Urushihara, T. Itoh, *SAE Trans.* paper 2006-01-1202 115 (3), 2006.
[35] R.E. Herold, J. Ghandi, *SAE* paper 2007-01-4044, 2007.
[36] B. Thirouard, J. Cherel, V. Knop, *SAE Trans.* paper 2005-01-0141 114 (3), 2005.
[37] J.-O. Olsson, P. Tunestål, B. Johansson et al., *SAE Trans.* paper 2002-01-0111 111 (3), 2002.
[38] M. Sjöberg, J.E. Dec, N.P. Cernansky, *SAE Trans.* paper 2005-01-0113 114 (3) (2005) 236–251.
[39] J.B. Heywood, *Internal Combustion Engine Fundamentals*, McGraw-Hill, New York, 1988.
[40] M. Sjöberg, J.E. Dec, *SAE Trans.* paper 2005-01-2125 114 (3) (2005) 1472–1486.
[41] M. Sjöberg, J.E. Dec, *Proc. Combst. Inst.* 31 (2007) 2895–2902.
[42] M. Sjöberg, J.E. Dec, *SAE* paper 2003-01-3173, 2003.
[43] J.E. Dec, M. Sjöberg, *SAE Trans.* paper 2004-01-0557 113 (4) (2004) 239–257.
[44] P. Risberg, G. Kalghatgi, H.-E. Ångström, *SAE* paper 2003-01-3215, 2003.
[45] G. Kalghatgi, *SAE* paper 2005-01-0239, 2005.

[46] G. Shibata, T. Urushihara, *SAE Trans.* paper 2007-01-0220 116 (3), 2007.
[47] H. Akagawa, T. Miyamoto, A. Harada et al., *SAE Trans.* paper 1999-01-0183 108 (3), 1999.
[48] M. Odaka, H. Suzuki, N. Koike, H. Ishii, *SAE Trans.* paper 1999-01-0184 108 (3), 1999.
[49] M. Sjöberg, J.E. Dec, *SAE Trans.* paper 2006-01-0629 115 (3) (2006) 318–334.
[50] W. Hwang, J.E. Dec, M. Sjöberg, *Combst. Flame* 154 (3) (2008) 387–409.
[51] P. Risberg, D. Johansson, J. Andrae, G. Kalghatgi, P. Björnbom, H.-E. Ångström, *SAE* paper 2006-01-0416, 2006.
[52] H. Yanagihara, Proceedings of the IFP International Congress on a New Generation of Engine Combustion Processes for the Future?, 2001, pp. 34–42.
[53] H. Yokota, Y. Kudo, H. Nakajima, T. Kakegawa, T. Suzuki, *SAE Trans.* paper 970891 106 (4), 1997.
[54] C.J. Mueller, G.C. Martin, T.E. Briggs, K.P. Duffy, *SAE Trans.* paper 2004-01-1843 113 (3), 2004.
[55] B. Walter, B. Gatellier, *SAE Trans.* paper 2002-01-1744 111 (4), 2002.
[56] Y. Sun, R.D. Reitz, *SAE* paper 2008-01-0058, 2008.
[57] K.P. Duffy, Proceedings of the 2004 Diesel Engine Emissions Reduction (DEER) Conference (2004), http://www1.eere.energy.gov/vehiclesandfuels/resources/proceedings/2004_deer_presentations.html.
[58] M. Sjöberg, J.E. Dec, W. Hwang, *SAE Trans.* paper 2007-01-0207 116 (3), 2007.
[59] W. de Ojeda, P. Zoldak, R. Espinosa, R. Kumar, *SAE* paper 2008-01-0057, 2008.
[60] X. He, R.P. Durrett, Z. Sun, *SAE* paper 2008-01-0637, 2008.
[61] Y. Murata, J. Kusaka, Y. Daisho et al., *SAE* paper 2008-01-0644, 2008.
[62] M. Weißbäk, J. Castó, M. Glensvig, T. Sams, P. Herzog, *MTZ Worldwide* 64 (9) (2003) 17–20.
[63] S. Kimura, O. Aoki, Y. Kitahara, E. Aiyoshizawa, *SAE Trans.* paper 2001-01-0200 110 (4), 2001.
[64] M.P.B. Musculus, *SAE Trans.* paper 2006-01-0079 115 (3), 2006.
[65] C.A. Idicheria, L.M. Pickett, *SAE Trans.* paper 2005-01-3834 114 (4), 2005.
[66] M.P.B. Musculus, T. Lachaux, L.M. Pickett, C.A. Idicheria, *SAE Trans.* paper 2007-01-0907 116 (3), 2007.
[67] J.T. Kashdan, N. Docquier, G. Bruneaux, *SAE Trans.* paper 2004-01-2945 113 (4), 2004.
[68] J.T. Kashdan, J.-F. Papagni, *SAE* paper 2005-01-3739, 2005.
[69] R. Collin, J. Nygren, M. Richter, M. Aldén, L. Hildingsson, B. Johansson, *SAE Trans.* paper 2004-01-2948 113 (4), 2004.
[70] C.L. Genzale, R.D. Reitz, M.P.B. Musculus, *SAE* paper 2008-01-1330, 2008.
[71] D. Kim, I. Ekoto, W.F. Colban, P.C. Miles, *SAE* paper 2008-01-1602, 2008.
[72] S. Singh, R.D. Reitz, M.P.B. Musculus, T. Lachaux, *Int. J. Engine Res.* 8 (1) (2007) 97–126.
[73] A. Hultqvist, M. Christensen, B. Johansson, A. Franke, M. Richter, M. Alden, *SAE Trans.* paper 1999-01-3680 108 (3), 1999.
[74] J.D. Naber, D.L. Siebers, *SAE Trans.* paper 960034 105 (3), 1996.
[75] W.F. Colban, P.C. Miles, S. Oh, *SAE Trans.* paper 2007-01-4063 116 (4), 2007.
[76] C. Noehre, M. Andersson, B. Johansson, A. Hultqvist, *SAE paper* 2006-01-3412, 2006.
[77] J. Yang, T. Culp, T. Kenney, *SAE Trans.* paper 2002-01-2832 111 (4), 2002.
[78] T. Urushihara, K. Hiraya, A. Kakuhou, T. Itoh, *SAE Trans.* paper 2003-01-0749 112 (3), 2003.
[79] L. Koopmans, R. Ogink, I. Denbratt, *SAE Trans.* paper 2003-01-1854 112 (4), 2003.
[80] N.B. Kaahaaina A.J. Simon, P.A. Caton, C.F. Edwards, *SAE Trans.* paper 2001-01-0549 110 (3), 2001.
[81] G.T. Kalghatgi, P. Risberg, H.-E. Ångström, *SAE Trans.* paper 2006-01-3385 115 (4), 2006.
[82] P.W. Bessonette, C.H. Schyler, K.P. Duffy, W.L. Hardy, M.P. Liechty, *SAE Trans.* paper 2007-01-0191 116 (3), 2007.